

Effect of the scalar unparticle and polarization at muon colliders through the exclusive W boson hadronic decays in the final state in the Randall-Sundrum model

Bui Thi Ha Giang^{a, 1}, Dang Van Soa^{b, 2}

^a Hanoi National University of Education, 136 Xuan Thuy, Hanoi, Vietnam

^b Faculty of Applied Sciences, University of Economics - Technology for Industries, 456 Minh Khai, Hai Ba Trung, Hanoi, Vietnam

Abstract

In this paper, by using Feynman diagram techniques we have evaluated the effect of the scalar unparticle and polarization at the muon colliders through the exclusive W boson hadronic decays $W^\pm \rightarrow \pi^\pm \gamma$, $W^\pm \rightarrow K^\pm \gamma$, $W^\pm \rightarrow \rho^\pm \gamma$ in the Randall-Sundrum (RS) model. The results show that with fixed collision energies, the total cross-sections for hadronic productions in final states depend strongly on the parameters of the unparticle physics and muon beam polarization. The total cross-sections achieve the maximum value when both of muon beams polarize left or right and the minimum value when the μ^- beam polarizes left, the μ^+ beam polarizes right and vice versa. In case of the different polarization, the cross-sections increase as the collision energy increases and they change insignificantly when the μ^- beam polarizes left, the μ^+ beam polarizes right. With the benchmark background $(\Lambda_U, d_U) = (1\text{TeV}, 1.9)$, the cross-sections reach the maximum value. The integrated luminosity value is shown to correspond to a significance $1\sigma, 3\sigma$.

Keywords: scalar unparticle, hadronic decay, muon collider.

I Introduction

After the discovery of the Higgs particle at the Large Hadron Collider (LHC) at CERN [1, 2], the particle content of the Standard Model (SM) has finally been completed. However, there are many open questions in physics that SM has yet to be address. One of the most attractive extended models beyond the SM is the Randall-Sundrum (RS) model [3]. The existence of an additional scalar called the radion (ϕ) is corresponded to the quantum fluctuations of the distance between the two three-branes: UV brane and IR brane. Radion and Higgs boson have the same quantum numbers. General covariance allows a possibility of mixing between the radion and the Higgs boson [4, 5]. In the Lagrangian of SM, the scale invariance is broken at or above the electroweak scale [6, 7]. At TeV scale, the scale invariant sector has been considered as an effective theory and that if it exists, it is made of unparticle suggested by Geogri [8, 9] and may become part of reality. Based on the Banks-Zaks theory [10, 11], unparticle stuff with nontrivial scaling dimension is considered to exist in our world and this opens a window to test the effects of the possible scalar invariant sector, experimentally. The effects of unparticle on properties of high energy colliders have been intensively studied in Refs. [12–23]. Dark matter and unparticles production in association with a Z boson in pp collisions at the center-of-mass energy 8 TeV has been considered in Ref. [24]. Recently, the scalar unparticle signals at LHC are studied in detail in Ref. [25]. The anomalous couplings at LHeC is researched in Ref. [26]. The muon colliders, which can reach center-of-mass energy up to tens of TeV, provide an unprecedented potential in probing new physics beyond the Standard Model [27]. The advantage of initial muon beam polarization is that it is effective for the indirect search [28, 29]. It is versatile in the fundamental particle physics and nuclear physics [30, 31]. The integrated luminosity scaling of a high

¹e-mail: giangbth@hnue.edu.vn, ORCID: 0000-0001-5814-0645 (corresponding author)

²e-mail: soadangvan@gmail.com, ORCID: 0000-0003-4694-7147 (corresponding author)

energy muon collider (assuming a 5 year run) reaches 1 ab^{-1} (3 TeV), 10 ab^{-1} (10 TeV) and 20 ab^{-1} (14 TeV) [32–35]. In our previous work, investigation of the scalar unparticle and anomalous couplings at muon colliders in final states with multiple photons in the RS model is considered in detail in Ref. [36]. The contribution of the scalar unparticle on the WW production at ILC is studied in Ref. [37] in which we only considered in s-channel without considering the influence of $\gamma WW, ZWW$ anomalous couplings and neutrino propagator. Moreover, rare hadronic decays of W bosons in the final states would provide an accurate measurement of the W boson mass that is based solely on visible decay products at future colliders [38–40]. These rare processes, if observed, would validate the quantum chromodynamics (QCD) factorization formalism used to calculate cross-sections at colliders [40].

In this work, by using the rare decay channels of W boson $W^\pm \rightarrow \pi^\pm \gamma$, $W^\pm \rightarrow K^\pm \gamma$, $W^\pm \rightarrow \rho^\pm \gamma$ we calculate in detail the cross-sections for hadronic production in the final states at muon colliders in the RS model. This paper is arranged as follows. The effect of the scalar unparticle and polarization at the muon colliders through the exclusive W boson hadronic decays are calculated in detail in Section II. Finally, we summarize our results and make conclusions in Section III.

II Effect of the scalar unparticle and polarization at the muon colliders through the exclusive W boson hadronic decays

Influence of unparticle and polarization on properties of high energy colliders have been intensively studied in Refs. [12–23]. The production of dark matter and unparticles associated with Z boson at 8 TeV via pp collisions has been analyzed in Ref. [24]. Recently, the scalar unparticle signals at LHC 14 TeV are investigated in Ref. [25]. Phenomenology of heavy neutral gauge boson at muon colliders are presented in detail in [41], which indicate that it can provide an unprecedented potential in probing new physics beyond the Standard Model.

Study for the exclusive boson hadronic decay with the ATLAS detector at 13 TeV is considered in detail in Ref. [40]. Recently, mass biases in reconstructing exclusive radiative hadronic decays of W boson at the LHC are given in Ref. [42]. Rare and exclusive few-body decays of the Higgs, Z and W bosons and the top quark are given in Ref. [43]. However, the influence of scalar unparticle and polarization at muon colliders through hadronic decays of W boson has not yet been invested. In this work, by using the rare decay channels of W boson $W^\pm \rightarrow \pi^\pm \gamma$, $W^\pm \rightarrow K^\pm \gamma$, $W^\pm \rightarrow \rho^\pm \gamma$ we calculate in detail the cross-sections for hadronic production at muon colliders.

Now we consider the collision process $\mu^+ \mu^- \rightarrow W^+ W^-$,

$$\mu^-(p_1) + \mu^+(p_2) \rightarrow W^-(k_1) + W^+(k_2). \quad (1)$$

The transition amplitude representing s-channel is given by

$$M_s = M_\gamma + M_Z + M_\phi + M_h + M_U, \quad (2)$$

where

$$M_\gamma = i \frac{e}{q_s^2} \bar{v}(p_2) \gamma^\sigma u(p_1) \eta_{\sigma\beta} \varepsilon_\mu^*(k_1) \Gamma_{WW\gamma}^{\beta\mu\nu} \varepsilon_\nu^*(k_2), \quad (3)$$

$$M_Z = -i \frac{g}{2\cos\theta_W (q_s^2 - m_Z^2)} \bar{v}(p_2) \gamma^\sigma \left(-\frac{1}{2} + 2\sin^2\theta_W - \frac{1}{2}\gamma_5 \right) u(p_1) \left(\eta_{\sigma\beta} - \frac{q_\sigma q_\beta}{m_Z^2} \right) \varepsilon_\mu^*(k_1) \Gamma_{WWZ}^{\beta\mu\nu} \varepsilon_\nu^*(k_2) \quad (4)$$

$$M_\phi = -i \frac{\bar{g}_{\mu\phi} \bar{g}_{W\phi}}{q_s^2 - m_\phi^2} \bar{v}(p_2) u(p_1) \varepsilon_\mu^*(k_1) [\eta^{\mu\nu} - 2g_\phi^W ((k_1 k_2) \eta^{\mu\nu} - k_1^\nu k_2^\mu)] \varepsilon_\nu^*(k_2), \quad (5)$$

$$M_h = -i \frac{\bar{g}_{\mu h} \bar{g}_{Wh}}{q_s^2 - m_h^2} \bar{v}(p_2) u(p_1) \varepsilon_\mu^*(k_1) [\eta^{\mu\nu} - 2g_h^W ((k_1 k_2) \eta^{\mu\nu} - k_1^\nu k_2^\mu)] \varepsilon_\nu^*(k_2), \quad (6)$$

$$M_U = i\bar{g}_{\mu\mu U}\bar{g}_{WWU}\frac{A_{d_U}}{2\sin(d_U\pi)}(-q_s^2)^{d_U-2}\bar{v}(p_2)u(p_1)\varepsilon_\mu^*(k_1)[(k_1k_2)\eta^{\mu\nu} - k_1^\nu k_2^\mu]\varepsilon_\nu^*(k_2), \quad (7)$$

Here, $q_s = p_1 + p_2 = k_1 + k_2$, $s = (p_1 + p_2)^2$ is the square of the collision energy, M_U is the contribution by the scalar unparticle, which is important for the described process. $\bar{g}_{\mu\mu\phi}, \bar{g}_{\mu\mu h}, \bar{g}_{W\phi}, \bar{g}_{Wh}$ are the couplings of Higgs/radion shown in Ref. [4]. $\bar{g}_{\mu\mu U}, \bar{g}_{WWU}, A_{d_U}$ are given by Ref. [7, 9]. Anomalous couplings are shown in Ref. [44] as follow

$$i\Gamma_{\mu\nu\lambda}^{WW\gamma}(p_1, p_2, p_3) = ie \left[T_{\mu\nu\lambda}^{(0)}(p_1, p_2, p_3) + \Delta k_\gamma T_{\mu\nu\lambda}^{(1)}(p_1, p_2, p_3) + \frac{\lambda_\gamma}{M_W^2} T_{\mu\nu\lambda}^{(2)}(p_1, p_2, p_3) \right], \quad (8)$$

$$i\Gamma_{\mu\nu\lambda}^{WWZ}(p_1, p_2, p_3) = ie \left[T_{\mu\nu\lambda}^{(0)}(p_1, p_2, p_3) + \Delta k_Z T_{\mu\nu\lambda}^{(1)}(p_1, p_2, p_3) + \frac{\lambda_Z}{M_W^2} T_{\mu\nu\lambda}^{(2)}(p_1, p_2, p_3) \right], \quad (9)$$

where the $T_{\mu\nu\lambda}$ tensors are, respectively,

$$T_{\mu\nu\lambda}^{(0)} = \eta_{\mu\nu}(p_1 - p_2)_\lambda + \eta_{\nu\lambda}(p_2 - p_3)_\mu + \eta_{\lambda\mu}(p_3 - p_1)_\nu, \quad (10a)$$

$$T_{\mu\nu\lambda}^{(1)} = \eta_{\lambda\mu}p_{3\nu} - \eta_{\nu\lambda}p_{3\mu}, \quad (10b)$$

$$T_{\mu\nu\lambda}^{(2)} = p_{1\lambda}p_{2\mu}p_{3\nu} - p_{1\nu}p_{2\lambda}p_{3\mu} - \eta_{\mu\nu}(p_2p_3p_{1\lambda} - p_3p_1p_{2\lambda}) - \eta_{\nu\lambda}(p_3p_1p_{2\mu} - p_1p_2p_{3\mu})\eta_{\mu\lambda}(p_1p_2p_{3\nu} - p_2p_3p_{1\nu}). \quad (10c)$$

The transition amplitude representing t-channel can be written as

$$M_t = -\frac{g^2}{2}\varepsilon_\nu^*(k_2)\bar{v}(p_2)\gamma^\mu\frac{1-\gamma^5}{2}\hat{q}_t\varepsilon_\mu^*(k_1)\gamma^\nu\frac{1-\gamma^5}{2}u(p_1). \quad (11)$$

The total cross-section for the whole process can be calculated as follow

$$\sigma_{\pi^-\pi^+\gamma\gamma} = \sigma(\mu^-\mu^+ \rightarrow W^+W^-) \times Br(W^- \rightarrow \pi^-\gamma)Br(W^+ \rightarrow \pi^+\gamma), \quad (12)$$

$$\sigma_{K^-K^+\gamma\gamma} = \sigma(\mu^-\mu^+ \rightarrow W^+W^-) \times Br(W^- \rightarrow K^-\gamma)Br(W^+ \rightarrow K^+\gamma), \quad (13)$$

$$\sigma_{\rho^-\rho^+\gamma\gamma} = \sigma(\mu^-\mu^+ \rightarrow W^+W^-) \times Br(W^- \rightarrow \rho^-\gamma)Br(W^+ \rightarrow \rho^+\gamma). \quad (14)$$

From the expressions of the differential cross-section [45]

$$\frac{d\sigma(\mu^-\mu^+ \rightarrow W^+W^-)}{d\cos\psi} = \frac{1}{32\pi s} \frac{|\vec{k}_1|}{|\vec{p}_1|} |M_{fi}|^2, \quad (15)$$

where $\psi = (\vec{p}_1, \vec{k}_1)$ is the scattering angle. The model parameters are chosen as $\lambda_{\mu\mu} = \lambda_{WW} = \lambda_0 = 1$, $m_h = 125$ GeV, $m_\phi = 125$ GeV, $\Lambda_\phi = 5$ TeV [26]. The integrated luminosity scaling of a high energy muon collider reaches $140 fb^{-1}$ at a center-of-mass energy of $\sqrt{s} = 13$ TeV [40]. The bounds on the anomalous $W^-W^+\gamma$ and W^-W^+Z couplings are provided by the LEP, Tevatron and LHC experiments. The ATLAS collaboration has updated the best available constraints on anomalous couplings $\Delta k_\gamma, \lambda_\gamma, \Delta k_Z, \lambda_Z$ obtained as follows: $\Delta k_\gamma \in [-0.135, 0.190]$, $\lambda_\gamma \in [-0.065, 0.061]$, $\Delta k_Z \in [-0.061, 0.093]$, $\lambda_Z \in [-0.062, 0.065]$ [46]. From the formulas (28 - 30) above and branching ratio of W boson in Ref. [40], we give estimates in detail for the cross-sections as follows:

i) In Fig.1, the total cross-sections are plotted as the function of P_{μ^-}, P_{μ^+} , which are the polarization coefficients of μ^-, μ^+ beams, respectively. The parameters are chosen as $d_U = 1.1$, $\Lambda_U = 1$ TeV [36], $\sqrt{s} = 13$ TeV. The figures indicate that the total cross-sections achieve the maximum values when $P_{\mu^-} = P_{\mu^+} = \pm 1$ and the minimum values when $P_{\mu^-} = 1, P_{\mu^+} = -1$ or $P_{\mu^-} = -1, P_{\mu^+} = 1$.

ii) The model parameters are chosen as in Fig.1. The polarization coefficients (P_{μ^-}, P_{μ^+}) are chosen as in Ref. [41], $(P_{\mu^-}, P_{\mu^+}) = (1, -1), (0.8, -0.8), (0.6, -0.6), (1, 1)$, respectively. The total cross-sections

in $\mu^+\mu^- \rightarrow W^+W^- \rightarrow \pi^-\pi^+\gamma\gamma/K^-K^+\gamma\gamma/\rho^-\rho^+\gamma\gamma$ collisions which depend on the collision energy are shown in Fig.2. From the figure we can see that the cross-sections increase when the collision energy increases. In case of μ^- beam is left polarized, μ^+ beam is right polarized and vice versa, the cross-sections change insignificantly.

iii) The total cross - section depends on $(\Delta k_\gamma, \lambda_\gamma)$ shown in the Fig.3. The parameters are chosen as $P_{\mu^-} = 0.8, P_{\mu^+} = -0.8, \sqrt{s} = 13$ TeV, $\Lambda_U = 1$ TeV, $d_U = 1.1, \Delta k_Z = 0.093, \lambda_Z = 0.065$. With the fixed value of Δk_γ , the cross-sections in $\mu^+\mu^- \rightarrow W^+W^- \rightarrow \pi^-\pi^+\gamma\gamma/K^-K^+\gamma\gamma/\rho^-\rho^+\gamma\gamma$ collisions are independent on λ_γ values. The result shows that cross-sections are the largest in the yellow region of the figures in which numerical values are given by (a) 2.9×10^{-4} fb, (b) 2.35×10^{-4} fb and (c) 2.2×10^{-3} fb in final states, respectively.

iv) The total cross - section depends on $(\Delta k_Z, \lambda_Z)$ shown in the Fig.4. The model parameters are chosen as in Fig.3, $P_{\mu^-} = 0.8, P_{\mu^+} = -0.8, \sqrt{s} = 13$ TeV, $\Lambda_U = 1$ TeV, $d_U = 1.1, \Delta k_\gamma = 0.190, \lambda_\gamma = 0.061$. The cross-sections in the yellow region of the figures are the largest with the values (a) 2.995×10^{-4} fb, (b) 2.395×10^{-4} fb and (c) 2.245×10^{-3} fb in final states, respectively.

v) We evaluate the benchmark background (Λ_U, d_U) in Fig.5. The parameters are chosen as above, $P_{\mu^-} = 0.8, P_{\mu^+} = -0.8, \sqrt{s} = 13$ TeV, $\Delta k_\gamma = 0.190, \lambda_\gamma = 0.061, \Delta k_Z = 0.093, \lambda_Z = 0.065$. From the figure, we can see that with $(\Lambda_U, d_U) = (1\text{TeV}, 1.9)$, the cross-sections in final states reach the maximum values. This result is similar to Ref. [25].

vi) For background, we choose the parameters as $P_{\mu^-} = 0.8, P_{\mu^+} = -0.8, \sqrt{s} = 13$ TeV, $\Delta k_\gamma = 0.190, \lambda_\gamma = 0.061, \Delta k_Z = 0.093, \lambda_Z = 0.065, \Lambda_U = 1$ TeV, $d_U = 1.1$. Using the integrated luminosity scaling of a high energy muon collider 140 fb^{-1} [40], some values $S/\sqrt{S+B}$ are given in Table.1. The results show that the pair production of mesons and photons can be detected with a small significance level. Therefore, we evaluate the integrated luminosity value correspond to $1\sigma, 3\sigma$ for the final states included scalar unparticle propagator in detail in Table.2. The cross-sections in the propagators are considered in detail in Table.3, which shows that the contribution of t-channel (neutrino propagator) is larger than that of s-channel under the same conditions. In case μ^- beam is left polarized, μ^+ beam is right polarized and vice versa, there is only the s-channel contribution. The forward-backward asymmetry A_{FB} values in case of the different polarization coefficients of μ^-, μ^+ beams are indicated in Table.4. At fixed collision energy and in case of $(P_{\mu^-}, P_{\mu^+}) = (1, -1), (0.8, -0.8), (0.6, -0.6), (1, 1)$, the forward-backward asymmetry A_{FB} is about 0.0050076, 0.000255, 0.000254, 0.000252, respectively.

III Conclusion

In this paper, by using Feynman diagram techniques we have evaluated the effect of the scalar unparticle and polarization at the muon colliders through the exclusive W boson hadronic decays in the RS model. The results show that with fixed collision energies, the total cross-sections for hadronic productions in final states depend strongly on the parameters of the unparticle physics and muon beam polarizes. The cross-sections achieve the maximum value when both of muon beams polarize left or right and the minimum value when the μ^- beam polarizes left, the μ^+ beam polarizes right and vice versa. In case of the different polarization, the cross section increases as the collision energy increases and it changes insignificantly when the μ^- beam polarizes left, the μ^+ beam polarizes right. With the benchmark background $(\Lambda_U, d_U) = (1\text{TeV}, 1.9)$, the cross-sections reach the maximum value. In our numerical estimation, the measured forward-backward asymmetry is quiet small which shows the direction to collect the final state from the experiment.

Finally, we emphasize that in this work we have only considered on a theoretical basis, other problems concerning experiments of exclusive boson hadronic decays, the reader can see in detail in Refs. [40, 42]. Note that these rare processes provide a test bench for the quantum chromodynamics

Table 1: $S/\sqrt{S+B}$ at 13 TeV muon collider with 140 fb^{-1} integrated luminosity.

Process	(P_{μ^-}, P_{μ^+})	σ_B (fb)	σ_S (fb)	$S/\sqrt{S+B}$
$\mu^+\mu^- \rightarrow W^+W^- \rightarrow \pi^-\pi^+\gamma\gamma$	(1, -1)	3.02273×10^{-13}	2.8179×10^{-7}	0.0062
	(0.8, -0.8)	0.00004	0.00029	0.1888
	(0.6, -0.6)	0.00007	0.00052	0.2533
	(1, 1)	0.00022	0.00164	0.4499
$\mu^+\mu^- \rightarrow W^+W^- \rightarrow K^-K^+\gamma\gamma$	(1, -1)	2.41986×10^{-13}	2.25589×10^{-7}	0.0056
	(0.8, -0.8)	0.00003	0.00023	0.1687
	(0.6, -0.6)	0.00005	0.00042	0.2292
	(1, 1)	0.00018	0.00131	0.4015
$\mu^+\mu^- \rightarrow W^+W^- \rightarrow \rho^-\rho^+\gamma\gamma$	(1, -1)	2.26412×10^{-12}	2.1107×10^{-6}	0.0172
	(0.8, -0.8)	0.00031	0.00221	0.5209
	(0.6, -0.6)	0.00054	0.00392	0.6945
	(1, 1)	0.00169	0.01226	1.2282

Table 2: The integrated luminosity value \mathcal{L} correspond to $1\sigma, 3\sigma$ for the final states included scalar unparticle propagator .

Process	(P_{μ^-}, P_{μ^+})	1σ	3σ
$\mu^+\mu^- \rightarrow W^+W^- \rightarrow \pi^-\pi^+\gamma\gamma$	(1, -1)	$3.54 \times 10^6 \text{ fb}^{-1}$	$3.19 \times 10^7 \text{ fb}^{-1}$
	(0.8, -0.8)	3923 fb^{-1}	35315 fb^{-1}
	(0.6, -0.6)	2182 fb^{-1}	19637 fb^{-1}
	(1, 1)	691 fb^{-1}	6224 fb^{-1}
$\mu^+\mu^- \rightarrow W^+W^- \rightarrow K^-K^+\gamma\gamma$	(1, -1)	$4.43 \times 10^6 \text{ fb}^{-1}$	$3.99 \times 10^7 \text{ fb}^{-1}$
	(0.8, -0.8)	4914 fb^{-1}	44234 fb^{-1}
	(0.6, -0.6)	2664 fb^{-1}	23979 fb^{-1}
	(1, 1)	868 fb^{-1}	7814 fb^{-1}
$\mu^+\mu^- \rightarrow W^+W^- \rightarrow \rho^-\rho^+\gamma\gamma$	(1, -1)	473777 fb^{-1}	$4.26 \times 10^6 \text{ fb}^{-1}$
	(0.8, -0.8)	516 fb^{-1}	4643 fb^{-1}
	(0.6, -0.6)	290 fb^{-1}	2612 fb^{-1}
	(1, 1)	93 fb^{-1}	835 fb^{-1}

factorization formalism used to calculate cross-sections at high energy colliders (the center-of-mass energy up to tens of TeV), as well as a probe of W boson coupling to quarks and a new way to measure the W boson mass through fully reconstructed decay products.

Acknowledgements: The work is supported in part by the National Foundation for Science and Technology Development (NAFOSTED) of Vietnam under Grant No. 103.01-2023.50.

Table 3: Cross-sections in the propagators at 13 TeV muon collider .

Process	(P_{μ^-}, P_{μ^+})	$\sigma_{\phi,h,U}$ (fb)	$\sigma_{\gamma,Z}$ (fb)	σ_ν (fb)
$\mu^+\mu^- \rightarrow W^+W^- \rightarrow \pi^-\pi^+\gamma\gamma$	(1, -1)	2.81791×10^{-7}	0	0
	(0.8, -0.8)	2.29137×10^{-7}	0.000031	0.000136
	(0.6, -0.6)	1.84141×10^{-7}	0.000055	0.000242
	(1, 1)	0	0.000172	0.000758
$\mu^+\mu^- \rightarrow W^+W^- \rightarrow K^-K^+\gamma\gamma$	(1, -1)	2.25589×10^{-7}	0	0
	(0.8, -0.8)	1.83436×10^{-7}	0.000025	0.000109
	(0.6, -0.6)	1.47415×10^{-7}	0.000044	0.000194
	(1, 1)	0	0.000139	0.000607
$\mu^+\mu^- \rightarrow W^+W^- \rightarrow \rho^-\rho^+\gamma\gamma$	(1, -1)	2.1107×10^{-6}	0	0
	(0.8, -0.8)	1.7163×10^{-6}	0.000235	0.001022
	(0.6, -0.6)	1.37928×10^{-6}	0.000418	0.001817
	(1, 1)	0	0.001307	0.005679

Table 4: Forward-backward asymmetry A_{FB} in case of the different polarization coefficients of μ^- , μ^+ beams.

\sqrt{s}	10 TeV	13 TeV	14TeV
$A_{FB} ((P_{\mu^-}, P_{\mu^+}) = (1, -1))$	0.005076	0.005076	0.005076
$A_{FB} ((P_{\mu^-}, P_{\mu^+}) = (0.8, -0.8))$	0.000255	0.000255	0.000255
$A_{FB} ((P_{\mu^-}, P_{\mu^+}) = (0.6, -0.6))$	0.000254	0.000254	0.000254
$A_{FB} ((P_{\mu^-}, P_{\mu^+}) = (1, 1))$	0.000252	0.000252	0.000252

References

- [1] Georges Aad et al. (ATLAS), *Phys. Lett.* **B716**, 1 (2012).
- [2] Serguei Chatrchyan et al. (CMS), *Phys. Lett.* **B716**, 30 (2012).
- [3] L. Randall and R. Sundrum, *Phys. Rev. Lett.* **83**, 3370 (1999).
- [4] A. Ahmed, B. M. Dillon, B. Grzadkowski, J. F. Gunion and Y. Jiang, *Phys. Rev.* **D95**, 095019 (2017).
- [5] D. Dominici, B. Grzadkowski, J. F. Gunion and M. Toharia, *Nucl.Phys.* **B671**, 243 (2003).
- [6] H. Zhang, C. S. Li and Z. Li, *Phys. Rev.* **D76**, 116003 (2007).
- [7] K. Cheung, W. Y. Keung and T. C. Yuan, *Phys. Rev. Lett.* **99**, 051803 (2007).
- [8] H. Georgi, *Phys. Rev. Lett.* **98**, 221601 (2007).
- [9] H. Georgi, *Phys. Lett.* **B650**, 275 (2007).
- [10] T. Banks and A. Zaks, *Nucl. Phys.* **B196**, 189 (1982).

- [11] S-L. Chen, X-G. He, *Phys. Rev.* **D76**, 091702 (2007).
- [12] P. Mathews and V. Ravindran, *Phys. Lett.* **B657**, 198 (2007).
- [13] A.T. Alan and N.K. Pak, *EPL* **84**, 1, 11001 (2008).
- [14] S. Majhi, *Phys. Lett.* **B665**, 44 (2008).
- [15] M.C. Kumar, P. Mathews, V.Ravindran and A.Tripathi, *Phys. Rev.* **D77**, 055013 (2008).
- [16] I. Sahin and B. Sahin, *Eur. Phys. J.* **C55**, 325 (2008).
- [17] T.Kikuchi and N.Okada, *Phys. Rev.* **D77**, 094012 (2008).
- [18] C. H. Chen, G. Cvetič, C. S. Kim, *Phys. Lett.* **B694**, 393 (2011).
- [19] S. Khatibi, M. M. Najafabadi, *Phys. Rev.* **D87**, 3, 037701 (2013).
- [20] A. Friedland, M. Giannotti, M. Graesser, *Phys. Lett.* **B678**, 149 (2009).
- [21] E. O. Iltan, *Eur. Phys. J.* **C56**, 105 (2008).
- [22] D. V. Soa and B. T. H. Giang, *Nucl. Phys.* **B936**, 1 (2018).
- [23] D. V. Soa *et al.*, *Mod. Phys. Lett.* **A27**, 1250126 (2012).
- [24] CMS Collaboration, *Phys. Rev.* **D93**, 052011 (2016).
- [25] T.M. Aliev, S. Bilmis, M. Solmaz and I. Turan, *Phys. Rev.* **D95**, 9, 095005 (2017).
- [26] B. T. H. Giang, *Chin. Phys.* **C47**, 2, 023108 (2023).
- [27] J. Blas , J. Gu, and Z. Liu, *Phys. Rev.* **D106**, 073007 (2022).
- [28] H. Fukuda, T. Moroi, A. Niki and S-F Wei, *JHEP* **02**, 214 (2024).
- [29] K. Korshynska, M. Löschner, M. Marinichenko, K. Mekała, J. Reuter, *Eur. Phys. J.* **C84**, 6, 568 (2024).
- [30] T. P. Gorringer and D. W. Hertzog, *Prog. Part. Nucl. Phys.* **84**, 73 (2015).
- [31] W. H. Breunlich, P. Kammel, J. S. Cohen, and M. Leon, *Rev. Nucl. Part. Sci.* **39**, 311 (1989).
- [32] P. Asadi, R. Capdevilla, C. Cesarotti, S. Homiller, *JHEP* **10**, 182 (2021).
- [33] R. Capdevilla, F. Meloni, R. Simoniello, J. Zurita *JHEP* **06**, 133 (2021).
- [34] A. Wulzer *et.al.*, *Eur. Phys. J.* **C83**, 864 (2023).
- [35] Z. Liu, K-F. Lyu, I. Mahbub, L-T. Wang, *Phys. Rev.* **D109**, 035021 (2024).
- [36] B. T. H. Giang, D. V. Soa, L. M. Dung, *I. J. Mod. Phys.* **A39**, 5& 6, 2450029 (2024).
- [37] D. V. Soa, B. T. H. Giang, *Mod. Phys. Lett* **A35**, 2050217 (2020).
- [38] A. M. Sirunyan (CMS Collaboration), *Phys. Rev. Lett.* **122**, 151802 (2019).
- [39] A. M. Sirunyan (CMS Collaboration), *Phys. Lett.* **B819**, 136409 (2021).

- [40] G. Aad *et al* (ALTA Collaboration), *Phys. Rev. Lett.* **133**, 161804 (2024).
- [41] Z. Lu, H. Li, Z-L. Han, Z-G. Si, and L. Zhao, *Sci.China Phys. Mech. Astron.* **67**, 3, 231012 (2024).
- [42] E.Jones and W.J. Murray, *New. J. Phys.* **23**, 11, 113035 (2021).
- [43] D. d'Enterria *et al*, *J. Phys. G: Nucl. Part. Phys.* in press <https://doi.org/10.1088/1361-6471/ad3c59> (2024).
- [44] D. Bhatia, U. Maitra, and S. Raychaudhuri, *Phys. Rev.* **D99**, 095017 (2019).
- [45] M. E. Peskin and D. V. Schroeder, *An Introduction to Quantum Field Theory*, Addison-Wesley Publishing (1995).
- [46] I.T. Cakir, O. Cakir, A. Senol, A. T. Tasci, *Acta Phys. Polon.* **B45**, 10, 1947 (2014).

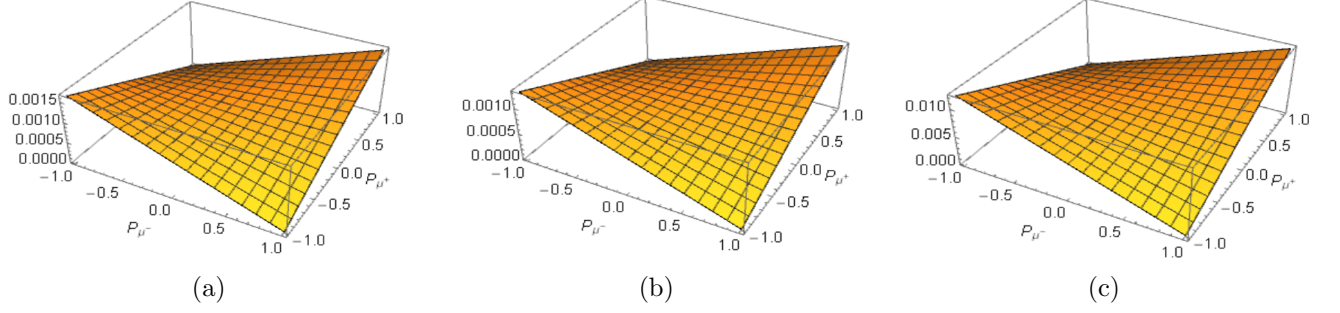


Figure 1: The total cross-section as a function of the polarization coefficients of muon and antimuon beam in (a) $\mu^+\mu^- \rightarrow W^+W^- \rightarrow \pi^-\pi^+\gamma\gamma$, (b) $\mu^+\mu^- \rightarrow W^+W^- \rightarrow K^-K^+\gamma\gamma$, (c) $\mu^+\mu^- \rightarrow W^+W^- \rightarrow \rho^-\rho^+\gamma\gamma$. The parameters are chosen as $\sqrt{s} = 13$ TeV, $\Lambda_U = 1$ TeV, $d_U = 1.1$, $\Delta k_\gamma = 0.190$, $\lambda_\gamma = 0.061$, $\Delta k_Z = 0.093$, $\lambda_Z = 0.065$.

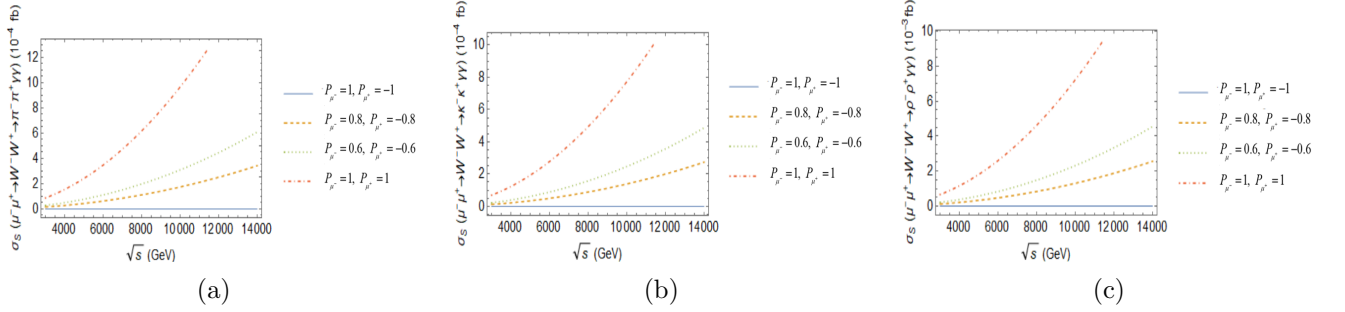


Figure 2: The total cross-section depends on the collision energy in (a) $\mu^+\mu^- \rightarrow W^+W^- \rightarrow \pi^-\pi^+\gamma\gamma$, (b) $\mu^+\mu^- \rightarrow W^+W^- \rightarrow K^-K^+\gamma\gamma$, (c) $\mu^+\mu^- \rightarrow W^+W^- \rightarrow \rho^-\rho^+\gamma\gamma$ collisions in case of $(P_{\mu^-}, P_{\mu^+}) = (1, -1), (0.8, -0.8), (0.6, -0.6), (1, 1)$. The parameters are chosen as $\Lambda_U = 1$ TeV, $d_U = 1.1$, $\Delta k_\gamma = 0.190$, $\lambda_\gamma = 0.061$, $\Delta k_Z = 0.093$, $\lambda_Z = 0.065$.

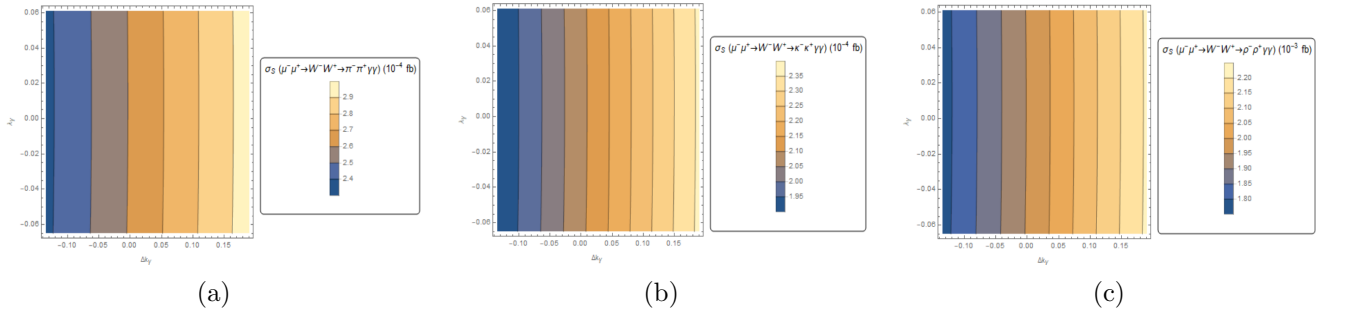


Figure 3: The total cross-section depends on the $(\Delta k_\gamma, \lambda_\gamma)$ in (a) $\mu^+\mu^- \rightarrow W^+W^- \rightarrow \pi^-\pi^+\gamma\gamma$, (b) $\mu^+\mu^- \rightarrow W^+W^- \rightarrow K^-K^+\gamma\gamma$, (c) $\mu^+\mu^- \rightarrow W^+W^- \rightarrow \rho^-\rho^+\gamma\gamma$ collisions. The parameters are chosen as $\sqrt{s} = 13$ TeV, $P_{\mu^-} = 0.8$, $P_{\mu^+} = -0.8$, $\Lambda_U = 1$ TeV, $d_U = 1.1$, $\Delta k_Z = 0.093$, $\lambda_Z = 0.065$.

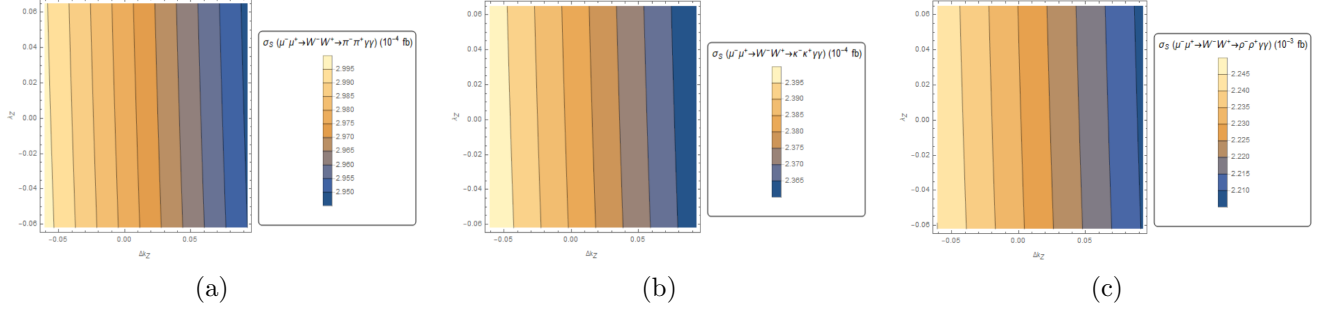


Figure 4: The total cross-section depends on the $(\Delta k_Z, \lambda_Z)$ in (a) $\mu^+\mu^- \rightarrow W^+W^- \rightarrow \pi^-\pi^+\gamma\gamma$, (b) $\mu^+\mu^- \rightarrow W^+W^- \rightarrow K^-K^+\gamma\gamma$, (c) $\mu^+\mu^- \rightarrow W^+W^- \rightarrow \rho^-\rho^+\gamma\gamma$ collisions. The parameters are chosen as $\sqrt{s} = 13$ TeV, $P_{\mu^-} = 0.8, P_{\mu^+} = -0.8, \Lambda_U = 1$ TeV, $d_U = 1.1, \Delta k_\gamma = 0.190, \lambda_\gamma = 0.061$.

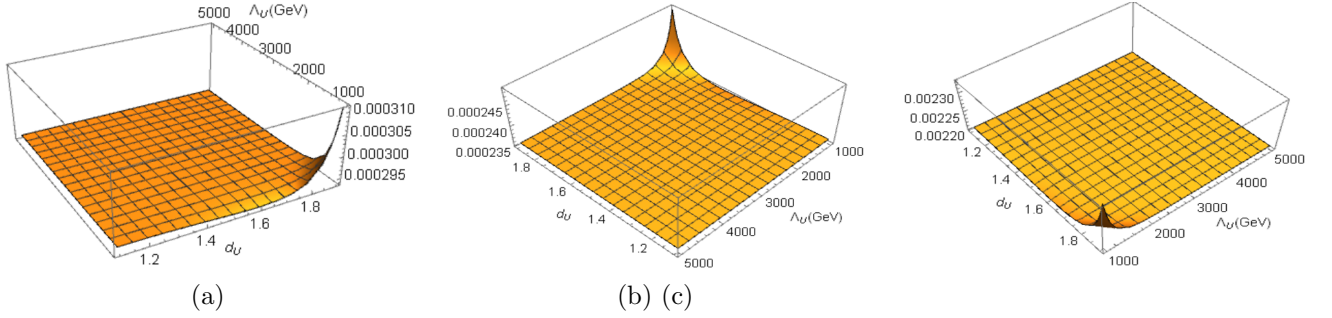


Figure 5: The total cross-section depends on the (Λ_U, d_U) in (a) $\mu^+\mu^- \rightarrow W^+W^- \rightarrow \pi^-\pi^+\gamma\gamma$, (b) $\mu^+\mu^- \rightarrow W^+W^- \rightarrow K^-K^+\gamma\gamma$, (c) $\mu^+\mu^- \rightarrow W^+W^- \rightarrow \rho^-\rho^+\gamma\gamma$ collisions. The parameters are chosen as $\sqrt{s} = 13$ TeV, $P_{\mu^-} = 0.8, P_{\mu^+} = -0.8, \Delta k_\gamma = 0.190, \lambda_\gamma = 0.061, \Delta k_Z = 0.093, \lambda_Z = 0.065$.

APPENDIX A: Feynman diagrams for the considered process

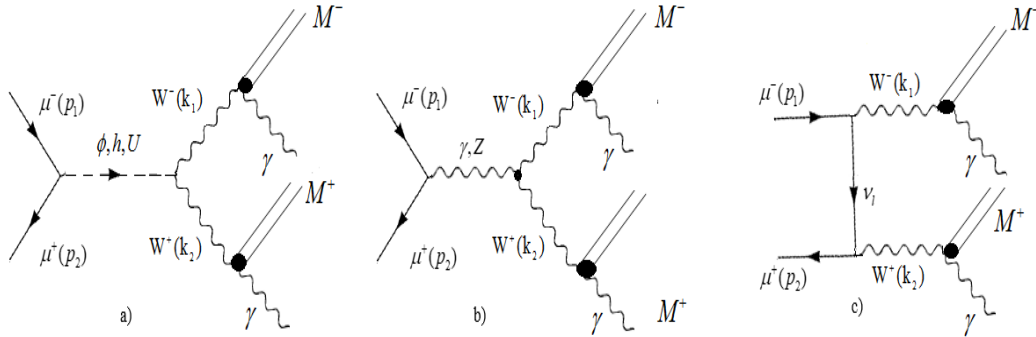


Figure 6: Feynman diagrams for $\mu^+\mu^- \rightarrow W^+W^- \rightarrow \pi^-\pi^+\gamma\gamma/K^-K^+\gamma\gamma/\rho^-\rho^+\gamma\gamma$ collisions. M^\pm stands for the π^\pm, K^\pm, ρ^\pm .